Chin. Phys. Lett. **39**, 070304 (2022)

Quench Dynamics of Bose–Einstein Condensates in Boxlike Traps

Rong Du(杜荣)[1], Jian-Chong Xing(邢健崇)[1], Bo Xiong(熊波)[2], Jun-Hui Zheng(郑俊辉)[1], and Tao Yang(杨涛)[1,3*]

[1]*Shaanxi Key Laboratory for Theoretical Physics Frontiers, Institute of Modern Physics, Northwest University, Xi'an 710127, China*
[2]*School of Science, Wuhan University of Technology, Wuhan 430070, China*
[3]*NSFC-SPTP Peng Huanwu Center for Fundamental Theory, Xi'an 710127, China*

(Received 16 April 2022; accepted manuscript online 31 May 2022)

By quenching the interatomic interactions, we investigate the nonequilibrium dynamics of two-dimensional Bose–Einstein condensates in boxlike traps with power-law potential boundaries. We show that ring dark solitons can be excited during the quench dynamics for both concave and convex potentials. The quench's modulation strength and the steepness of the boundary are two major factors influencing the system's evolution. In terms of the number of ring dark solitons excited in the condensate, five dynamic regimes have been identified. The condensate undergoes damped radius oscillation in the absence of ring dark soliton excitations. When it comes to the appearance of ring dark solitons, their decay produces interesting structures. The excitation patterns for the concave potential show a nested structure of vortex-antivortex pairs. The dynamic excitation patterns for the convex potential, on the other hand, show richer structures with multiple transport behaviors.

DOI: 10.1088/0256-307X/39/7/070304

Nonequilibrium dynamics is a hot topic in science, with applications ranging from the early universe to condensed matter physics. New quantum physics such as Mott transitions,[1] synthetic gauge fields,[2] and topological states[3,4] have been discovered in driven systems far away from equilibrium. Because of its high tunability in experiments, the Bose–Einstein condensate (BEC) is an excellent platform to study nonequilibrium quantum dynamics. The temporal evolution following a sudden or slow change of the coupling constants of the system Hamiltonian, known as quantum quenches, has piqued researchers' interest.[5] Recently, an abrupt change of the scattering length was achieved experimentally.[6], Many fascinating nonequilibrium dynamics, such as the formation of matter-wave solitons, are involved in tuning interatomic interaction in atomic BECs,[7−10] the transformation between different types of vector solitons,[11] controlled collapse,[12] Faraday patterns,[13] collective excitation modes[14,15] and matter-wave jet emission.[16−19]

Solitons give researchers a way to investigate the nonlinear properties of interacting Bose gases. These important topological excitations are closely related to nonlinear optics,[20,21] superfluidity,[22,23] and superconductivity.[24] They can be created in trapped BECs by phase imprinting via carefully controlled laser fields,[25−27] controlling the condensate density via creating shock waves,[28] or colliding separated condensates.[29−31] Recently, quench of the isotropic s-wave scattering length was employed to prepare solitons in quasi-one-dimensional box-trapped BECs.[32] The stability of dark solitons under nonresonant $\mathcal{PT}$-symmetric pumping was studied in Ref. [33]. A nonlinear Bloch equation has been shown to govern the motion of solitons in one-dimensional BECs under spin-orbit coupling.[34] Dark solitons and vortices are linked in higher dimensions where dark solitons are prone to breaking up due to transverse (snaking) instability,[35] resulting in the emergence of vortices spontaneously. In two-dimensional (2D) systems of interest, the ring dark soliton (RDS) is a unique structure. The decay of single ring dark soliton (S-RDS) initially sitting in the condensate has been studied.[36−38] In Ref. [39] the dynamics and modulation of RDSs in 2D BECs with tunable interaction were investigated. The interplay of double RDS (D-RDS) initially seeded in a condensate cloud was found to be unstable, resulting in the formation of complex multi-vortex-lattice configurations.[40] To excite RDSs in trapped 2D BECs, a sudden quench of the harmonic well into a wider cylindrical well was proposed.[41]

Furthermore, the trapping geometries have a significant impact on the trapped BECs' dynamics. Traps with either hard or soft boundaries can be achieved, such as harmonic traps, hard-wall box potentials,[42] and soft wall potential with power-law boundaries, which can be achieved with the advancement of experimental technologies.[43] When a matter-

*Corresponding author. Email: yangt@nwu.edu.cn
© 2022 Chinese Physical Society and IOP Publishing Ltd

wave dark soliton incident upon a hard-wall potential, a significant fraction of its energy is emitted.[44] The quantum reflection of matter-wave bright solitons from a soft wall with a positive tanh potential is very sensitive to the width of the potential.[45] In a one-dimensional hard-wall box potential, the nonlinear Talbot effect of BEC can occur.[46] The formation of large-scale Onsager vortex clusters is prevalent in steep-walled traps, but suppressed in harmonic traps, according to numerical studies.[47,48] There are numerous studies on 2D dark solitons in BECs using various traps.[49–55]

In this Letter, the effect of a sudden quench of the interatomic interaction on the nonequilibrium dynamics of a 2D BEC confined in various types of power-law traps is investigated. We identify five dynamic regimes based on the ability of exciting RDSs in the system and depict the phase diagram with respect to the modulation strength and steepness of the boundary. The system undergoes low-lying breathing mode[56] with damped oscillation of the radius of the condensate for relatively weak modulations of interatomic interaction. RDSs are excited and develop into different patterns of vortex pairs, depending on the convexity and concavity of the trap's boundary for a stronger tuning.

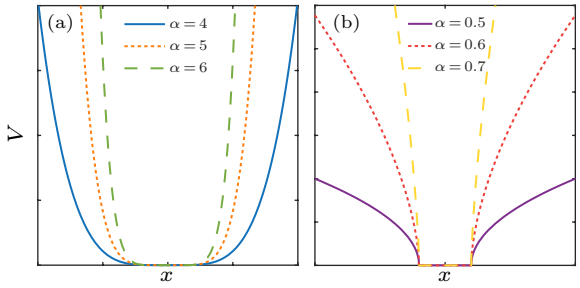

Fig. 1. Schematic side view ($y = 0$) of power-law traps with different exponents α: (a) concave potentials with $\alpha > 1$ for $w = 0.4$ and $b = 2$, (b) convex potentials with $0 < \alpha < 1$ for $w = 1.2$ and $b = 0.0002$.

We consider a condensate confined in a cylindrically symmetric boxlike trap to investigate the trap's boundary. The boundary of the trap increases as the form's spatial coordinate increases in power,[57]

$$V(\boldsymbol{r}) = \begin{cases} 0, & r \le w, \\ \left(\frac{r-w}{b}\right)^{\alpha}, & r > w, \end{cases} \tag{1}$$

with $r = \sqrt{x^2 + y^2}$. Two crossing blue-detuned Laguerre–Gaussian optical beams can be used to create such a trap in the lab.[58] As is known, w and b can be utilized to adjust the width of the flat part of the potential and the relative width of the potential boundary, respectively. The exponent α denotes the steepness of the boundary, i.e., the sharp spatial variation of the boxlike trap's edge potential. For $\alpha > 1$, the boundary of the potential is concave, while for $0 < \alpha < 1$ the boundary of the potential is convex as shown in Fig. 1. The trap tends to be an infinite square well with width $2(w+b)$ as $\alpha \to \infty$, and a finite square well with width $2w$ when $\alpha \to 0$. The Gross–Pitaevskii (GP) equation describes the dynamics of a 2D BEC with N atoms,

$$i\hbar\frac{\partial\psi}{\partial t} = -\frac{\hbar^2}{2\,m}\nabla^2\psi + V(\mathbf{r})\psi + c(t)gN|\psi|^2\psi, \tag{2}$$

where $g = 2\sqrt{2\pi}\hbar\omega_z a_s a_z$ is the effective interatomic interaction strength with a_s being the s-wave scattering length and $a_z = \sqrt{\hbar/m\omega_z}$ being the characteristic length in z direction. We choose $a_s = 5.4$ nm and $m = 1.44 \times 10^{-25}$ kg, appropriate to a ^{87}Rb condensate. The trap frequency ω_z in the z direction is set to be $2\pi \times 100$ Hz to make sure that $\hbar\omega_z$ is much larger than the chemical potential of the system. The ground state of the condensate with the modulation factor $c = 1$ trapped in the given boxlike potential with soft-wall boundaries, which can be obtained by the imaginary time evolution, is the initial state of the system. The nonequilibrium dynamics is triggered by an instantaneous quench of the interatomic interaction by changing c which causes an instantaneous quench of the interatomic interaction. Feshbach resonances can be used to achieve this.[59] In the following calculation, we set $\omega_0 = 2\pi \times 5$ Hz and use $a_0 = \sqrt{\hbar/m\omega_0}$, $t_0 = 1/\omega_0$, and $E_0 = \hbar\omega_0$ as units of length, time, and energy, respectively. All physical parameters in this study are presented in dimensionless forms.

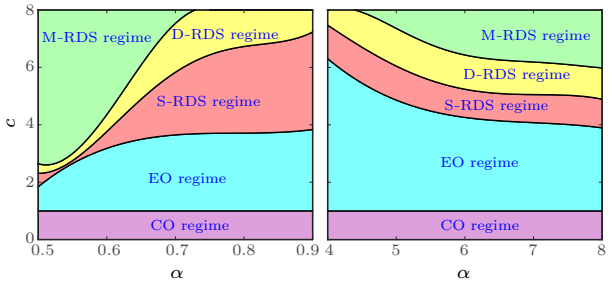

Fig. 2. Phase diagram describing the dynamic regimes of the ground-state BEC suddenly quenched from (α, g) to (α, cg). Five dynamic regimes, i.e., compressing oscillating (CO), expanding oscillating (EO), single ring dark soliton (S-RDS), double ring dark solitons (D-RDS), and multiple ring dark solitons (M-RDS) are indicated in different colors.

We identify five dynamical regimes for each given α based on the ability to generate RDSs for both concave and convex potentials, as shown in the dynamic phase diagram (Fig. 2). We can see that the phase boundaries are strongly influenced by the steepness of the trap's boundary. The boundary ($c = 1$) serves as a reference line, indicating the initial interaction strength before quench. The reduced interatomic interaction causes the condensate cloud to compress to

a minimum radius and then expand when the modulation factor c is set to $0 < c < 1$. The breathing mode induced by the quench is the oscillation of the radius of the condensate. After the condensate is reflected by the boundary, ring-shaped self-interference patterns are excited during this dynamic process. We label this regime as compressing oscillating (CO) regime. In Fig. 3(a), we show the typical density profile of the condensate in the CO regime at $t = 1.25$. The radius oscillation of the condensate is shown in Fig. 3(b), where the red stars are numerical data and the blue solid line is the fitting curve $R(t) = 2.88 + 0.25\exp(-0.06\,t)\cos(5.3\,t)$. For $c > 1$, the quench dynamics can also display a breathing mode. The size oscillation of the condensate in this case, however, begins with an increasing radius, which is labeled as expanding oscillating (EO) regime. As shown in Fig. 3(c), due to the stronger interatomic interaction in the real-time evolution, the induced density oscillations in the EO regime are much stronger than those in the CO regime. The radius oscillation of the condensate is fitted by the blue solid line $R(t) = 3.9892 - 0.7\exp(-0.7\,t)\cos(8.243\,t)$ in Fig. 3(d). The damping rate and the oscillation frequency are both larger than those in the CO regime and the system quickly settles into a steady state. There are no topological excitations in the system in these two regimes. With increasing c, the quench process triggers the formation of S-RDS, D-RDS, and multiple ring dark solitons (M-RDS). On α, the boundaries of the dynamic phases exhibit opposite monotonic behavior depending on the trap potential's convexity and concavity, as shown in Fig. 2. Moreover, the subsequent decay of the RDS(s) exhibits distinct mechanisms.

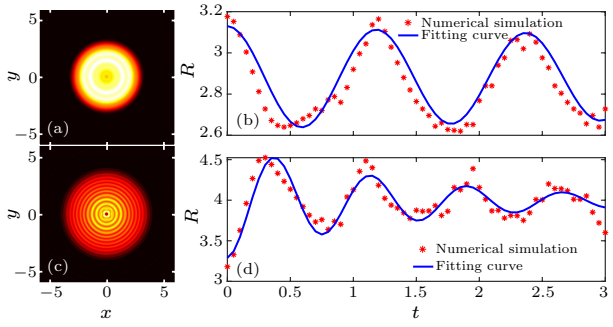

Fig. 3. Hot-scale plots of atom density (white = high) and radius oscillation of the condensate: [(a), (b)] $\alpha = 4$ and $c = 0.4$, [(c), (d)] $\alpha = 4$ and $c = 5$. Here $w = 0.4$ and $b = 2$.

For the concave potential with $\alpha = 4$, one dynamic RDS is excited in the system [see Fig. 4(a1)] with c tuned from 1 to 6.4 suddenly (S-RDS regime). As shown in Figs. 4(d) and 4(e), the RDS locates in the innermost shell of the concentric density rings, which is identified by both the density notch and a phase jump at $x = 0.67$. All of the other fringes are ring-shaped density wave oscillations with a slow and smooth change in the condensate phase. The velocity of the condensate flow is proportional to the gradient of the phase, $v_s \propto \nabla\theta$, so a sharp phase variation means a large superfluid velocity [see Fig. 4(f)].

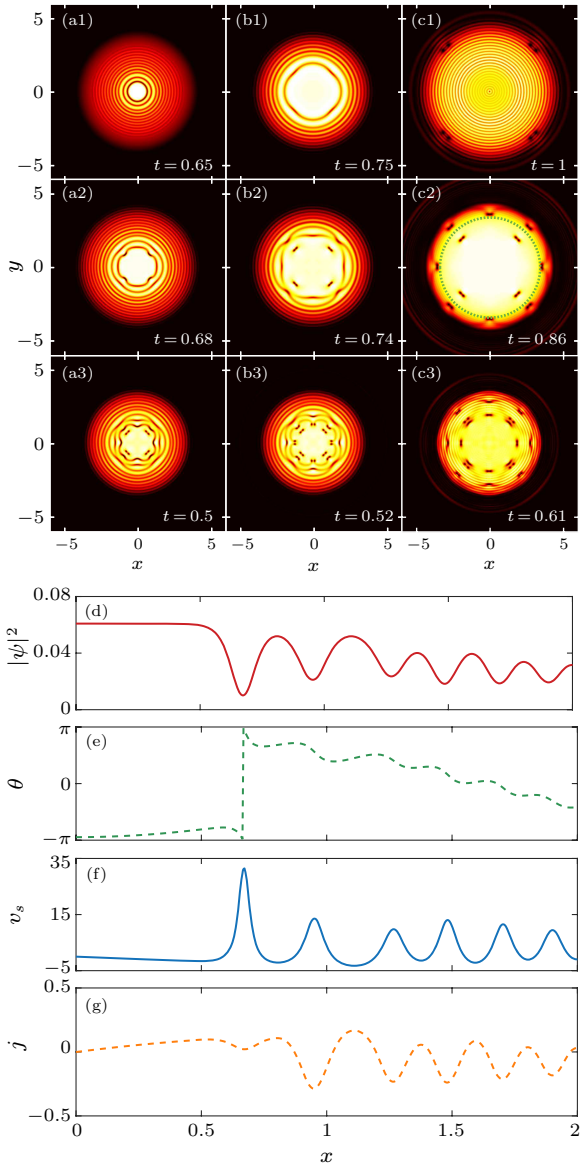

Fig. 4. (a1)–(c3) Hot-scale plots of atom density (white = high). The parameters (α, c) are (4, 6.4), (4, 7.8), and (5, 7.6) for (a), (b), and (c), respectively. (d)–(g) The corresponding radial distributions of the density, phase, velocity and particle current of (a1), respectively. Here $w = 0.4$ and $b = 2$.

However, the low density induces rather flat and small particle current distribution $j(r) = |\psi(r)|^2 v_s(r)$ near the RDS [see Fig. 4(g)]. As a result, density oscillations are absent in the condensate in the RDS-encircled regime [see Figs. 4(a1), 4(b1) and 4(d)]. Eventually, the RDS decays into four vortex-antivortex pairs via snake instability during its expansion toward the periphery of the condensate [see

Figs. 4(b1) and 4(c1)]. The decay process is identical to that described in Ref. [36] for the RDS originally imprinted in the harmonically trapped condensate. For a given radius of the RDS, the number of vortex pairs produced is proportional to the original depth of the input soliton, but always in multiples of four.[36] The depth of an RDS is related to the phase modulation across the soliton, and the number of vortex pairs excited depends on the radius of the RDS for a given initial depth. A larger radius may excite more pairs.

As shown in Fig. 4(a2), in the D-RDS regime, two concentric rings with low density appear at the center of the condensate cloud after c is quenched from 1 to 7.8. Because their locations coincide well with phase jumps, these two rings are referred to as RDSs. The inner RDS is deeper and begins snaking earlier than the outer one, indicating that splitting is imminent. Then it decays into four vortex pairs in $\times$-type configuration [see Fig. 4(b2)], similar to what happened in [Fig. 4(c1)]. However, there are four additional lumps in the $+$ direction that are rapidly approaching the condensate's rim. The outer RDS begins to decay into four vortex pairs at the same time [see Fig. 4(b2)]. The remaining lumps of the inner RDS will not annihilate in the rim of the condensate due to the existence of the outer RDS, but will instead turn into four more vortex pairs. The twelve vortex pairs then arrange themselves in three layers, forming a nested structure in the $\times-+-\times$ configuration [see Fig. 4(c2)]. Layer structure of vortices has been identified in the collapse of RDSs in a two-component BEC.[60]

For $\alpha = 5$, if we tune c from 1 to 7.6, the dynamics of the system enter the M-RDS regime. In Figs. 4(a3), 4(b3), and 4(c3), three RDSs are excited and then decay into 20 vortex pairs. The outermost RDS splits into four vortex pairs, while the other two split into eight. If there are n RDSs excited during the quench, then they will decay into $4 + 8(n-1)$ vortex pairs. The initial distribution of these pairs right after the complete decay of the RDSs is the nested periodic $\times-+-\times-\cdots$ configuration as shown in Fig. 4(c3).

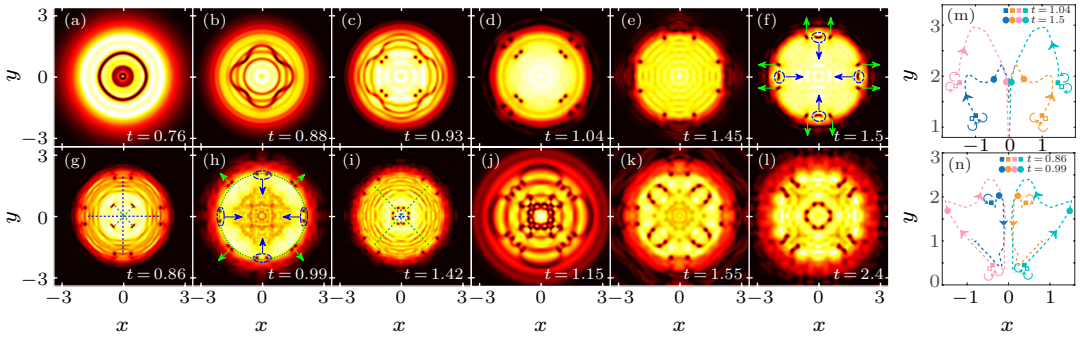

Fig. 5. Hot-scale plots of atom density (white = high) and typical vortex trajectories. (a)–(f) D-RDS regime with $\alpha = 0.6$ and $c = 4.2$. (g)–(h) D-RDS regime with $\alpha = 0.7$ and $c = 7.2$. (i) D-RDS regime with $\alpha = 0.7$ and $c = 7$. (j)–(l) M-RDS regime with $\alpha = 0.55$ and $c = 4$. Here $w = 1.2$ and $b = 0.0002$. The blue and green arrows indicate the directions of the vortex pair movements. (m) The vortex trajectories depict the vortices' penetration between the layers. (n) The vortex trajectories show the crisscross of the vortices between the layers. The solid squares and solid circles represent the positions of the vortices at various times. The hollow squares are the positions of the counterparts of the vortices indicated by the solid squares.

The dynamics of the system trapped in the convex potential in the S-RDS regime are very similar to those of the system trapped in the concave potential. The RDS decay into four vortex pairs. The average density of the condensate in the convex potential is higher than that in the concave potential for the same number of atoms. As a result, the radius of the RDS excited could be smaller. When more than one RDS are exited in the system with a convex trap, however, the dynamical excitation pattern has much richer structures. We choose a set of typical parameters with $\alpha = 0.6$ and $c = 4.2$ to drive the system into the D-RDS regime. With density and phase analysis, we can confirm that there are only two RDSs excited [see Fig. 5(a)]. The outer ring does not expand much, but it bends heavily before the deformation of the inner ring, which is an interesting fact [Fig. 5(b)]. When compared to the concave case, the dynamics are quite different. Instead of snaking, the inner RDS expands while maintaining its circular shape. After interacting with the outer RDS, eight vortex pairs in the parallel $\times$-type configuration are excited in the condensate [Figs. 5(c) and 5(d)]. Then the vortices and antivortices from these pairs move along the rings in two layers and rearrange themselves into the parallel $+$-type configuration [Fig. 5(e)]. We note that these double layers of parallel vortex-antivortex pairs occur in energy higher than that of the nested vortex pairs.

We also discovered typical mechanisms of evolution between layers of vortex pairs, such as penetration and crisscrossing. For the parallel layers of vortex pairs, the quartets of vortex pairs in the outer layer

can penetrate through the pairs of vortex and antivortex in the inner layer when they drift inward to the center of the condensate [Fig. 5(f)]. When the quartets of vortex pairs in the inner layer drift outward to the rim of the condensate, they can pass through the vortex and antivortex pairs in the outer layer. Around the rim of the condensate, a transient structure with an array of four linearly aligned vortex quadruples appears. For the nested layers, the vortex pairs in two layers move toward each other along the × and + directions [Figs. 5(g)], respectively, and then generate crisscross trajectories and a necklace of vortex pairs around the rim of the condensate [Fig. 5(h)]. The corresponding trajectories are shown in Figs. 5(m) and 5(n). The existence of the nested +–× and ×–+ configurations in the D-RDS regime is shown in Figs. 5(g) and 5(i).

The configurations appearing during the dynamics in the M-RDS regime can be even more complicated [Fig. 5(j)]. For $\alpha = 0.55$ and $c = 4$, there are three RDSs excited. The system will oscillate between some typical configurations of 12 vortex pairs in three layers after a period of evolution [Figs. 5(k) and 5(l)]. We find the hybrid configuration of parallel and nested structures. It is worth noting that vortex recombination can happen between layers as well.

After the decay of RDS(s), a transient stage appears during the evolution of vortex pairs in both concave and convex potentials, where a necklace of eight vortices (vortex pairs) is set along a single ring (or an octagon structure). For eight vortices [see Fig. 4(c1)], they will recombine themselves from +-type into ×-type vortex-antivortex pairs and vice versa. This is similar to the recombination of a vortex quadruple along the x and y directions.[61] However, for eight vortex pairs [see Fig. 5(h)], no recombination occurs between pairs from different layers (resulting from the decay of different RDSs).

Finally, we investigate the interaction-quench dynamics and excitation patterns of 2D BEC confined in boxlike traps with various kinds of power-law boundaries numerically. Excitations with different numbers of RDS have been observed depending on the modulation strength. For $\alpha \to 0$ or $\alpha \to \infty$, it is easier to excite RDSs in the system. For $\alpha \in [0.5, 0.6]$, the parameter regions of S-RDS and D-RDS are extremely narrow, indicating that the condensate is very sensitive to the interaction quench. D-RDS and M-RDS induced by quench dynamics have decay behaviors that are generally different from RDSs created by phase imprinting in the condensate. Moreover, their decay dynamics strongly depend on the concavity and convexity of the trap boundary. The decay of dynamic RDSs in a concave trap follows a universal rule. The inner RDS always splits into eight vortex pairs, while the outmost RDS decays into four pairs. Typical configurations such as × type, + type, and their nested structures are found. Richer structures of the vortex, such as parallel and nested × and + types, and their hybridization, are developed for a convex trap. In the quench dynamics in concave traps, concentric ring-shaped wave matter jets have been observed and the smaller α is, the easier to excite jets [see Figs. 4(c1)–4(c3)].

Acknowledgments. This work was supported by the National Natural Science Foundation of China (Grant Nos. 12175180, 11934015, and 11775178), the Major Basic Research Program of Natural Science of Shaanxi Province (Grant Nos. 2017KCT-12 and 2017ZDJC-32), and the Double First-Class University Construction Project of Northwest University.

References

[1] Eckardt A 2017 *Rev. Mod. Phys.* **89** 011004
[2] Dalibard J, Gerbier F, Juzeliūnas G and Öhberg P 2011 *Rev. Mod. Phys.* **83** 1523
[3] Jotzu G, Messer M, Desbuquois R, Lebrat M, Uehlinger T, Greif D and Esslinger T 2014 *Nature* **515** 237
[4] Mo L H, Zhang Q L and Wan X 2020 *Chin. Phys. Lett.* **37** 060301
[5] Polkovnikov A, Sengupta K, Silva A and Vengalattore M 2011 *Rev. Mod. Phys.* **83** 863
[6] Makotyn P, Klauss C E, Goldberger D L, Cornell E A and Jin D S 2014 *Nat. Phys.* **10** 116
[7] Khaykovich L, Schreck F, Ferrari G, Bourdel T, Cubizolles J, Carr L D, Castin Y and Salomon C 2002 *Science* **296** 1290
[8] Nguyen J H V, Luo D and Hulet R G 2017 *Science* **356** 422
[9] Carr L D and Brand J 2004 *Phys. Rev. A* **70** 033607
[10] Zong F D and Zhang J F 2008 *Chin. Phys. Lett.* **25** 2370
[11] Liu X, Pu H, Xiong B, Liu W M and Gong J 2009 *Phys. Rev. A* **79** 013423
[12] Abdullaev F K, Caputo J G, Kraenkel R A and Malomed B A 2003 *Phys. Rev. A* **67** 013605
[13] Staliunas K, Longhi S and de Valcárcel G J 2002 *Phys. Rev. Lett.* **89** 210406
[14] Pollack S E, Dries D, Hulet R G, Magalh A K M F, Henn E A L, Ramos E R F, Caracanhas M A and Bagnato V S 2010 *Phys. Rev. A* **81** 053627
[15] Vidanović I, Balaž A, Al-Jibbouri H and Pelster A 2011 *Phys. Rev. A* **84** 013618
[16] Clark L W, Gaj A, Feng L and Chin C 2017 *Nature* **551** 356
[17] Fu H, Feng L, Anderson B M, Clark L W, Hu J, Andrade J W, Chin C and Levin K 2018 *Phys. Rev. Lett.* **121** 243001
[18] Wu Z and Zhai H 2019 *Phys. Rev. A* **99** 063624
[19] Mežnaršič T, Žitko R, Arh T, Gosar K, Zupanič E and Jeglič P 2020 *Phys. Rev. A* **101** 031601
[20] Kivshar Y S and Luther-Davies B 1998 *Phys. Rep.* **298** 81
[21] Kivshar Y S, Christou J, Tikhonenko V, Luther-Davies B and Pismen L M 1998 *Opt. Commun.* **152** 198
[22] Kivotides D, Barenghi C F and Samuels D C 2000 *Science* **290** 777
[23] Bai W K, Yang T and Liu W M 2020 *Phys. Rev. A* **102** 063318
[24] Kopnin N B 2002 *Rep. Prog. Phys.* **65** 1633
[25] Burger S, Bongs K, Dettmer S, Ertmer W, Sengstock K,

Sanpera A, Shlyapnikov G V and Lewenstein M 1999 *Phys. Rev. Lett.* **83** 5198
[26] Denschlag J, Simsarian J E, Feder D L, Clark C W, Collins L A, Cubizolles J, Deng L, Hagley E W, Helmerson K, Reinhardt W P, Rolston S L, Schneider B I and Phillips W D 2000 *Science* **287** 97
[27] Fritsch A R, Lu M, Reid G H, Pi N A M and Spielman I B 2020 *Phys. Rev. A* **101** 053629
[28] Dutton Z, Budde M, Slowe C and Hau L V 2001 *Science* **293** 663
[29] Weller A, Ronzheimer J P, Gross C, Esteve J, Oberthaler M K, Frantzeskakis D J, Theocharis G and Kevrekidis P G 2008 *Phys. Rev. Lett.* **101** 130401
[30] Yang T, Xiong B and Benedict K A 2013 *Phys. Rev. A* **87** 023603
[31] Xiong B, Yang T and Benedict K A 2013 *Phys. Rev. A* **88** 043602
[32] Halperin E J and Bohn J L 2020 *Phys. Rev. Res.* **2** 043256
[33] Jia C Y and Liang Z X 2020 *Chin. Phys. Lett.* **37** 040502
[34] Wen L, Sun Q, Chen Y, Wang D S, Hu J, Chen H, Liu W M, Juzeliūnas G, Malomed B A and Ji A C 2016 *Phys. Rev. A* **94** 061602
[35] Kivshar Y S and Pelinovsky D E 2000 *Phys. Rep.* **331** 117
[36] Theocharis G, Frantzeskakis D J, Kevrekidis P G, Malomed B A and Kivshar Y S 2003 *Phys. Rev. Lett.* **90** 120403
[37] Wang W, Kevrekidis P G, Carretero-González R, Frantzeskakis D J, Kaper T J and Ma M 2015 *Phys. Rev. A* **92** 033611
[38] Song S W, Wang D S, Wang H and Liu W M 2012 *Phys. Rev. A* **85** 063617
[39] Hu X H, Zhang X F, Zhao D, Luo H G and Liu W M 2009 *Phys. Rev. A* **79** 023619
[40] Wang W, Kolokolnikov T, Frantzeskakis D J, Carretero-González R and Kevrekidis P G 2021 *Phys. Rev. A* **104** 023314
[41] Yang S J, Wu Q S, Zhang S N, Feng S, Guo W, Wen Y C and Yu Y 2007 *Phys. Rev. A* **76** 063606
[42] Gaunt A L, Schmidutz T F, Gotlibovych I, Smith R P and Hadzibabic Z 2013 *Phys. Rev. Lett.* **110** 200406
[43] Jaouadi A, Gaaloul N, de Viaris L B, Telmini M, Pruvost L and Charron E 2010 *Phys. Rev. A* **82** 023613
[44] Parker N G, Proukakis N P, Leadbeater M and Adams C S 2003 *J. Phys. B At. Mol. Opt. Phys.* **36** 2891
[45] Cornish S L, Parker N G, Martin A M, Judd T E, Scott R G, Fromhold T M and Adams C S 2009 *Phys. D Nonlinear Phenom.* **238** 1299
[46] Ruostekoski J, Kneer B, Schleich W P and Rempe G 2001 *Phys. Rev. A* **63** 043613
[47] Simula T, Davis M J and Helmerson K 2014 *Phys. Rev. Lett.* **113** 165302
[48] Groszek A J, Simula T P, Paganin D M and Helmerson K 2016 *Phys. Rev. A* **93** 043614
[49] Huang G, Makarov V A and Velarde M G 2003 *Phys. Rev. A* **67** 023604
[50] Baizakov B B, Malomed B A and Salerno M 2006 *Phys. Rev. E* **74** 066615
[51] Cheng Q L, Bai W K, Zhang Y Z, Xiong B and Yang T 2019 *Laser Phys.* **29** 015501
[52] Zhang X F, Hu X H, Wang D S, Liu X X and Liu W M 2011 *Front. Phys. Chin.* **6** 46
[53] Wang D M, Xing J C, Du R, Xiong B and Yang T 2021 *Chin. Phys. B* **30** 120303
[54] Verma G, Rapol U D and Nath R 2017 *Phys. Rev. A* **95** 043618
[55] Haberichter M, Kevrekidis P G, Carretero-González R and Edwards M 2019 *Phys. Rev. A* **99** 053619
[56] Yang T, Henning A J and Benedict K A 2014 *J. Phys. B: At. Mol. Opt. Phys.* **47** 035302
[57] Sciacca M, Barenghi C F and Parker N G 2017 *Phys. Rev. A* **95** 013628
[58] Clifford M A, Arlt J, Courtial J and Dholakia K 1998 *Opt. Commun.* **156** 300
[59] Chin C, Grimm R, Julienne P and Tiesinga E 2010 *Rev. Mod. Phys.* **82** 1225
[60] Wang L X, Dai C Q, Wen L, Liu T, Jiang H F, Saito H, Zhang S G and Zhang X F 2018 *Phys. Rev. A* **97** 063607
[61] Yang T, Hu Z Q, Zou S and Liu W M 2016 *Sci. Rep.* **6** 29066